Spin and cyclotron energies of electrons in GaAs/Ga$_{1-x}$Al$_x$As quantum wells

P. Pfeffer[*] and W. Zawadzki

Institute of Physics, Polish Academy of Sciences, Aleja Lotnikow 32/46, 02-668 Warsaw, Poland
(Received 10 March 2006; published 15 September 2006)

A five-level $\mathbf{P} \cdot \mathbf{p}$ model of the band structure for GaAs-type semiconductors is used to describe the spin g^* factor and the cyclotron mass m_c^* of conduction electrons in GaAs/Ga$_{1-x}$Al$_x$As quantum wells in an external magnetic field parallel to the growth direction [001]. It is demonstrated that the previous theory of the g^* factor in heterostructures is inadequate. Our approach is based on an iteration procedure of solving 14 coupled differential $\mathbf{P} \cdot \mathbf{p}$ equations. The applicability of the iteration procedure is verified. The final eigenenergy problem for the conduction subbands is reduced to two differential equations for the spin-up and spin-down states of consecutive Landau levels. It is shown that the bulk inversion asymmetry of III-V compounds is of importance for the spin g^* factor. Our theory with no adjustable parameters gives an excellent description of experimental data on the electron spin g^* factor in GaAs/Ga$_{0.67}$Al$_{0.33}$As rectangular quantum wells for different well widths between 3 and 21 nm. The same theory describes very well experimental cyclotron masses in GaAs/Ga$_{0.74}$Al$_{0.26}$As quantum wells for the well widths between 6 and 37 nm.

I. INTRODUCTION

Spin properties of electrons in semiconductor heterostructures have become in recent years the subject of intense experimental and theoretical interest because of their inherent scientific value as well as possible spintronic applications. Among numerous heterostructures, the system GaAs/Ga$_{1-x}$Al$_x$As has won a unique position. First, GaAs is, after silicon, the most important semiconductor material. Second, the system GaAs/Ga$_{1-x}$Al$_x$As has well-established parameters which allows the theorists to describe new subtle phenomena. Third, due to the advanced growth technology the electrons in GaAs quantum wells have very high mobilities making it possible to detect even weak effects. Thus it is of interest to describe precisely the spin and orbital electron energies in GaAs/Ga$_{1-x}$Al$_x$As quantum wells not only for their own sake, but also as a model example for other heterostructures. From the theoretical point of view, a description of magneto-optical effects in GaAs-type materials is not an easy task since GaAs is a medium gap semiconductor. As a result, its band structure exhibits features characteristic of narrow-gap materials, but it is insufficient to treat them by the models normally used for such systems. We showed in our previous work on bulk GaAs and InP that the simplest adequate description of the band structure of these materials is given by the so-called five-level $\mathbf{P} \cdot \mathbf{p}$ model.[1,2] Thus, the present work on the spin g^* factor of electrons in GaAs/Ga$_{1-x}$Al$_x$As quantum wells was first motivated by the fact that the theoretical description used in the literature for this purpose had been based on the three-level model.[3] Examining the problem we realized that the theory[3] suffers from other deficiencies, as we will demonstrate below. The theory we develop for the spin energies is equally valid for the cyclotron (orbital) energies, so that we describe also the cyclotron masses, although here our treatment improves only slightly the existing approach.[4]

An important feature of the III-V compounds is a bulk inversion asymmetry (BIA) of these materials. As is known

from the fifties,[5] the BIA results in a spin splitting of energies for a given direction of the wave vector $\mathbf{k}$. It is, however, of interest to investigate how this spin splitting behaves in the presence of an external magnetic field. One can rephrase the problem by asking how the Zeeman spin splitting caused by the magnetic field combines with the spin splitting caused by BIA. In the bulk magneto-optical or magnetotransport studies one is usually interested in the Landau levels at $k_z = 0$, since the density of Landau states has singularities at the vanishing k_z. However, in a quantum well one deals with electric subbands for which the value of k_z^2 is "frozen" in the subband wave function along the growth direction. The BIA splitting is sensitive to this k_z^2 value which increases with a decreasing well width. This in turn is reflected in the spin g^* factor. In the following we will be concerned with symmetric quantum wells, so that the Bychkov-Rashba spin splitting, caused by the structure inversion asymmetry, does not come into play.[6]

Our calculation of the spin and cyclotron electron energies in GaAs/Ga$_{1-x}$Al$_x$As heterostructures is based on the five-level $\mathbf{P} \cdot \mathbf{p}$ model (5LM). An important advantage of the model is that it includes the BIA mechanism of the spin splitting. We solve the eigenenergy problem by an iteration procedure which is more precise than an expansion in powers of momentum used in the literature. We check the precision of consecutive iteration steps. The results are compared with those obtained by the three-level $\mathbf{P} \cdot \mathbf{p}$ model (3LM) and it is shown that the latter is insufficient for the GaAs-type materials.

Our paper is organized as follows. In Sec. II the $\mathbf{P} \cdot \mathbf{p}$ theory within 5LM is formulated for the bulk semiconductor. Next the 3LM model is used to obtain results for the spin g^* value. It is demonstrated that the procedure of Ref. 3 based on the same model is inadequate. The iteration solution of 5LM is checked against "exact" results for the bulk, as obtained by a numerical procedure. In Sec. III the theory for the quantum wells is worked out from the 5LM matrix. Results for the spin g^* factor and the cyclotron mass are presented,
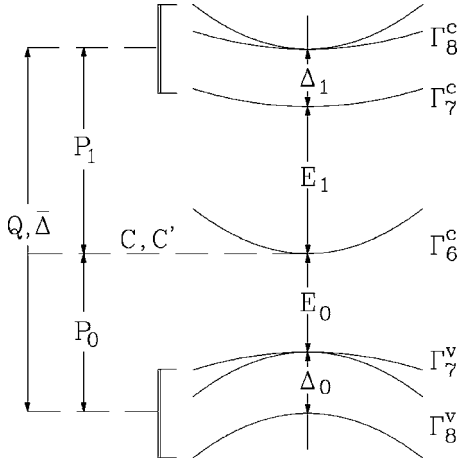
FIG. 1. Five-level model for the band structure of GaAs-type semiconductors. Energy gaps, spin-orbit energies, interband matrix elements of momentum, and of the spin-orbit interaction are indicated. Letters C and C' mark symbolically far-band contributions to the effective mass and the spin g^* factor of conduction electrons, respectively.

compared with experimental data and discussed in Sec. IV. The paper is concluded by a summary.

II. P·p THEORY

In order to discuss the previous treatments and to establish standards of precision for various approximations we first consider the three-dimensional (3D) case. The **P**·**p** theory, which is the **k**·**p** theory generalized for the presence of an external magnetic field **B**, has the form (cf. Ref. 1)

$$\sum_l \left[\left(\frac{P^2}{2m_0} + E^{(l)} - \mathcal{E} \right) \delta_{l'l} + \frac{1}{m_0} \mathbf{p}_{l'l} \cdot \mathbf{P} + \mu_B \mathbf{B} \cdot \boldsymbol{\sigma}_{l'l} + H^{so}_{l'l} \right] f_l$$

$$= 0, \qquad (1)$$

where $\mathcal{E}$ is the energy, $\mathbf{P} = \mathbf{p} + e\mathbf{A}$ is the kinetic momentum, **A** is the vector potential of magnetic field **B**, and $\boldsymbol{\sigma}_{l'l} = (1/\Omega)\langle u_{l'}|\boldsymbol{\sigma}|u_l\rangle$. Here $\boldsymbol{\sigma}$ are the Pauli spin matrices, Ω is the volume of the unit cell, u_l are periodic amplitudes of the Lüttinger-Kohn functions, $\mu_B = e\hbar/2m_0$ is the Bohr magneton, $\mathbf{p}_{l'l}$ are the interband matrix elements of momentum, and $H^{so}_{l'l}$ are those of spin-orbit interaction. The sum in Eq. (1) runs over all bands $l = 1, 2, \ldots$, included in the model, $l' = 1, 2, \ldots$, runs over the same bands, and $E^{(l)}$ are the band-edge energies, see below.

In the following we shall be concerned with the five-level model of the band structure, as illustrated in Fig. 1. Within this model there exist three interband matrix elements of momentum

$$P_0 = \frac{-i\hbar}{m_0\Omega} \langle S|p_x|X\rangle, \qquad (2)$$

$$P_1 = \frac{-i\hbar}{m_0\Omega} \langle S|p_x|X'\rangle, \qquad (3)$$

$$Q = \frac{-i\hbar}{m_0\Omega} \langle X|p_y|Z'\rangle = \frac{i\hbar}{m_0\Omega} \langle X'|p_y|Z\rangle, \qquad (4)$$

and three matrix elements of the spin-orbit interaction

$$\Delta_0 = \frac{-3i\hbar}{4m_0^2 c^2} \langle X|[\boldsymbol{\nabla}V_0, \mathbf{p}]_y|Z\rangle, \qquad (5)$$

$$\Delta_1 = \frac{-3i\hbar}{4m_0^2 c^2} \langle X'|[\boldsymbol{\nabla}V_0, \mathbf{p}]_y|Z'\rangle, \qquad (6)$$

$$\bar{\Delta} = \frac{-3i\hbar}{4m_0^2 c^2} \langle X|[\boldsymbol{\nabla}V_0, \mathbf{p}]_y|Z'\rangle, \qquad (7)$$

where the nonprimed functions are related to the Γ_7^v, Γ_8^v valence bands, while the primed functions are related to the Γ_7^c, Γ_8^c conduction bands. The band-edge energies $E^{(l)}$ are generally influenced by $\bar{\Delta}$ (cf. Ref. 1) but in GaAs-type materials, where $\bar{\Delta}$ is small, this feature may be ignored and we have $E^{(1)} = E^{(2)} = E^{(8)} = E^{(9)} = G_1 = E_1 + \Delta_1$; $E^{(3)} = E^{(10)} = E_1$; $E^{(5)} = E^{(6)} = E^{(12)} = E^{(13)} = E_0$; $E^{(7)} = E^{(14)} = G_0 = E_0 + \Delta_0$. We take the zero of energy at the Γ_6^c conduction band edge. Within 5LM there are 14 basis functions and the **P**·**p** differential Hamiltonian for the envelope functions $f_l(\mathbf{r})$ has the explicit form of Eq. (8). We define $P_0' = P_0/\hbar$, $P_1' = P_1/\hbar$, $Q' = Q/\hbar$, $\lambda = \mathcal{E} - \hbar\omega_c^0(a^+a + \frac{1}{2}) - p_z^2/2m_0$. Here $\omega_c^0 = eB/m_0$ is the cyclotron frequency with free-electron mass. The quantities $fb^\pm = C[\hbar\omega_c^0(a^+a + \frac{1}{2}) + p_z^2/2m_0] \pm C'\mu_B B$ result from the far-band contributions to the conduction band energies. The operators $P_\pm = (P_x \pm iP_y)/\sqrt{2}$ are proportional to the raising and lowering operators for the harmonic oscillator functions: $P_+ = -(\hbar/L)a^+$ and $P_- = -(\hbar/L)a$, in which $L = (\hbar/eB)^{1/2}$ is the magnetic radius. The matrices A_1, A_2, and D have different forms for various directions of magnetic field. In the following we shall be concerned with the case $\mathbf{B} \parallel [001]$ crystal direction, for which

$$
\begin{bmatrix}
G_1+\frac{\mu}{3}-\lambda & 0 & -(\sqrt{8}/3)\mu & 1/\sqrt{3}P_1'P_- & & 0 & 0 & 0 & -\sqrt{\tfrac{2}{3}}P_1'P_z \\
 & G_1-\mu-\lambda & 0 & -P_1'P+ & A_1 & 0 & 0 & 0 & 0 & & D \\
 & & E_1-\frac{\mu}{3}-\lambda & \sqrt{\tfrac{2}{3}}P_1'P_- & & 0 & 0 & 0 & 1/\sqrt{3}P_1'P_z \\
 & & & fb^--\mu-\lambda & 1/\sqrt{3}P_0'P_+ & -P_0'P_- & \sqrt{\tfrac{2}{3}}P_0'P_+ & \sqrt{\tfrac{2}{3}}P_1'P_z & 0 & -1/\sqrt{3}P_1'P_z & 0 & \sqrt{\tfrac{2}{3}}P_0'P_z & 0 & -1/\sqrt{3}P_0'P_z \\
 & & & & E_0+\frac{\mu}{3}-\lambda & 0 & -(\sqrt{8}/3)\mu & & -\sqrt{\tfrac{2}{3}}P_0'P_z & 0 & 0 & 0 \\
 & & & & & E_0-\mu-\lambda & 0 & -D & & 0 & 0 & 0 & 0 \\
 & & & & & & G_0-\frac{\mu}{3}-\lambda & & 1/\sqrt{3}P_0'P_z & 0 & 0 & 0 \\
 & & & & & & & G_1-\frac{\mu}{3}-\lambda & 0 & (\sqrt{8}/3)\mu & 1/\sqrt{3}P_1'P_+ \\
 & & & & & & & & G_1+\mu-\lambda & 0 & P_1'P_- & & A_2 \\
 & & & & & & & & & E_1+\frac{\mu}{3}-\lambda & \sqrt{\tfrac{2}{3}}P_1'P_+ \\
 & & & & & & & & & & fb^++\mu-\lambda & 1/\sqrt{3}P_0'P_- & P_0'P_+ & \sqrt{\tfrac{2}{3}}P_0'P_- \\
 & & & & & & & & & & & E_0-\frac{\mu}{3}-\lambda & 0 & (\sqrt{8}/3)\mu \\
 & & & & & & & & & & & & E_0+\mu-\lambda & 0 \\
 & & & & & & & & & & & & & G_0+\frac{\mu}{3}-\lambda
\end{bmatrix}
\tag{8}
$$

$$A_1 = A_2 = \begin{bmatrix} \frac{1}{3}\bar{\Delta} & \frac{1}{\sqrt{3}}Q'P_z & 0 \\ -\frac{1}{\sqrt{3}}Q'P_z & \frac{1}{3}\bar{\Delta} & -\sqrt{\frac{2}{3}}Q'P_z \\ 0 & \sqrt{\frac{2}{3}}Q'P_z & -\frac{2}{3}\bar{\Delta} \end{bmatrix}, \quad (9)$$

$$D = \begin{bmatrix} 0 & -\sqrt{\frac{2}{3}}Q'P_- & Q'P_+ \\ -\sqrt{\frac{2}{3}}Q'P_- & 0 & \sqrt{\frac{1}{3}}Q'P_- \\ -Q'P_+ & \sqrt{\frac{1}{3}}Q'P_- & 0 \end{bmatrix}. \quad (10)$$

For $Q=0$ and $k_z=0$ matrix (8) factorizes into two 7×7 matrices containing spin-up and spin-down electron energies. For $Q = 0$ and $k_z \neq 0$ the resulting bands are spherical (i.e., the energies do not depend on the direction of **B**), but the spin-up and spin-down states are mixed by the k_z terms. Still, in this case one can find solutions of the eigenvalue problem in the form of single harmonic oscillator functions. If $Q \neq 0$, the resulting bands are nonspherical and the above simple solutions do not exist. At this point we emphasize that matrix (8) contains no approximations within 5LM.

For considerations of the bulk there is no external potential. To describe the magnetic field we take the gauge $\mathbf{A}=[-By,0,0]$, corresponding to $\mathbf{B}\|[001]$. One can then look for the envelope functions in the form $f_l = \exp(ik_x x + ik_z z)\Phi_l(y)$, where $\Phi_l(y)$ are the harmonic oscillator functions.

A. Three-level model

The three-level model of Γ_6^c, Γ_7^v, Γ_8^v levels (see Fig. 1) is not adequate for the description of the conduction band in GaAs-type materials (see Refs. 1 and 2), but it can be solved exactly and we use it as a starting point of our considerations as well as for a discussion of the existing work on the g^* values.

Once the higher conduction levels are omitted, the couplings P_1, Q, and $\bar{\Delta}$ do not come into play (see Fig. 1), the conduction band is spherical, and the resulting 8×8 Hamiltonian may be solved in terms of eight harmonic oscillator functions. This was first done by Bowers and Yafet,[7] see also Refs. 8 and 9. In our more general formulation (8), the 3LM corresponds to considering the columns and rows 4, 5, 6, 7, 11, 12, 13, and 14. The resulting energy for the spin-up state of the nth Landau level is given by

$$\mathcal{E} = \hbar\,\omega_c^0\left(n + \frac{1}{2}\right)\left[1 + C - \frac{E_{P_0}}{3}\left(\frac{3}{2E_1^0} + \frac{1}{2E_3^0} + \frac{1}{G_2^0}\right)\right]$$
$$+ \frac{1}{2}\mu_B B\left[2 + 2C' + \frac{2E_{P_0}}{3}\left(\frac{3}{2E_1^0} - \frac{1}{2E_3^0} - \frac{1}{G_2^0}\right)\right]$$
$$+ \frac{\hbar^2 k_z^2}{2m_0}\left[1 + C - \frac{E_{P_0}}{3}\left(\frac{2}{E_2^0} + \frac{1}{G_1^0}\right)\right], \quad (11)$$

while the energy for the spin-down state of the nth Landau level is given by

$$\mathcal{E} = \hbar\,\omega_c^0\left(n + \frac{1}{2}\right)\left[1 + C - \frac{E_{P_0}}{3}\left(\frac{3}{2E_4^0} + \frac{1}{2E_2^0} + \frac{1}{G_1^0}\right)\right]$$
$$- \frac{1}{2}\mu_B B\left[2 + 2C' + \frac{2E_{P_0}}{3}\left(\frac{3}{2E_4^0} - \frac{1}{2E_2^0} - \frac{1}{G_1^0}\right)\right]$$
$$+ \frac{\hbar^2 k_z^2}{2m_0}\left[1 + C - \frac{E_{P_0}}{3}\left(\frac{2}{E_3^0} + \frac{1}{G_2^0}\right)\right], \quad (12)$$

where

$$E_1^0 = E_0 + \mu_B B + \hbar\omega_c^0\left(n - \frac{1}{2}\right) - \mathcal{E},$$

$$E_2^0 = E_0 + \frac{1}{3}\mu_B B + \hbar\omega_c^0\left(n - \frac{1}{2}\right) - \mathcal{E},$$

$$E_3^0 = E_0 - \frac{1}{3}\mu_B B + \hbar\omega_c^0\left(n + \frac{3}{2}\right) - \mathcal{E},$$

$$E_4^0 = E_0 - \mu_B B + \hbar\omega_c^0\left(n + \frac{3}{2}\right) - \mathcal{E},$$

$$G_1^0 = G_0 - \frac{1}{3}\mu_B B + \hbar\omega_c^0\left(n - \frac{1}{2}\right) - \mathcal{E},$$

$$G_2^0 = G_0 + \frac{1}{3}\mu_B B + \hbar\omega_c^0\left(n + \frac{3}{2}\right) - \mathcal{E}. \quad (13)$$

The first terms in Eqs. (11) and (12) represent the orbital parts, the second are related to the spin parts (they differ in sign for spin-up and spin-down states), and the third give k_z^2 parts for the motion along the magnetic field. Equations (11) and (12) represent fourth-order polynomials for the unknown energies. If we neglect the free-electron and far-band contributions, Eqs. (11) and (12) reduce to cubic equations for the energies. An influence of free-electron terms on the description of spin g^* factors in selected materials was discussed by Singh *et al.*[10]

In investigations of bulk semiconductors one is usually interested in the simplified case of $k_z = 0$ since the singular density of states for the Landau levels corresponds to the vanishing k_z. However, our final aim in this work is to investigate quantum wells, which corresponds to the situation of $k_z \neq 0$. Solving Eqs. (11) and (12) for the spin-up and spin-down energies one can find the cyclotron effective mass and the spin g^* value exactly within 3LM. We define the cyclotron mass m_c^* and the spin g^* value in the standard way

$$\mathcal{E}_{n+1}^{\pm} - \mathcal{E}_n^{\pm} = \frac{\hbar eB}{m_c^*}, \quad (14)$$

$$\mathcal{E}_n^+ - \mathcal{E}_n^- = \mu_B g^* B. \quad (15)$$

The dependence of m_c^* and g^* on the electron energy was established in the early days, see Refs. 11 and 12. Knowing the solutions of Eqs. (11) and (12) and fixing magnetic field intensity B one can determine the dependence of m_c^* and g^* on k_z^2 exactly within 3LM.

Since the conduction band in GaAs is only weakly nonparabolic, we can expand the exact energies using Eqs. (11) and (12) in the limit $\mathcal{E}/E_0 \ll 1$. The zero-order terms give m_0^* and g_0^* values at the conduction band edge. The first-order terms give the first nonparabolic approximation. One can alternatively say that the zero-order terms are proportional to

P_0^2 while the first-order terms are proportional to P_0^4. Using Eqs. (11) and (12) and the definitions (14) and (15) we obtain after some manipulation (we keep the free-electron terms and the far-band contributions only in the conduction band)

$$\frac{1}{m_c^*} = \frac{1}{m_0^*}\left[1 - \frac{E_{P_0}}{3}D_{nk_z}\left(\frac{1}{G_0^2}+\frac{2}{E_0^2}\right)\right], \qquad (16)$$

$$g^* = g_0^* + D_{nk_z}\frac{E_{P_0}}{3}\left[\frac{2m_0}{m_0^*}\left(\frac{1}{E_0^2}-\frac{1}{G_0^2}\right) \right.$$
$$\left. - g_0^*\left(\frac{1}{G_0^2}+\frac{2}{E_0^2}\right)\right], \qquad (17)$$

where $D_{nk_z}=\hbar\omega_c^0(n+1/2)+\hbar^2 k_z^2/2m_0$, and

$$\frac{m_0}{m_0^*} = 1 + C - \frac{E_{P_0}}{3}\left(\frac{2}{E_0}+\frac{1}{G_0}\right), \qquad (18)$$

$$g_0^* = 2 + 2C' + \frac{2E_{P_0}}{3}\left(\frac{1}{E_0}-\frac{1}{G_0}\right), \qquad (19)$$

are the band-edge values of the effective mass and of the g^* factor according to 3LM. We define $E_{P_0}=2m_0 P_0^2/\hbar^2$. To calculate the numerical values we take the following band parameters for GaAs: $E_{P_0}=27.865$ eV, $E_0=-1.519$ eV, $G_0=-1.86$ eV, $C=-3.070$, and $C'=-0.102$. This results in $m_0^*=0.0660m_0$ (Ref. 2) and $g_0^*=-0.44$.[13]

We would like to plot the g^* value as a function of energy in view of the applications to quantum wells (QW). To this end we calculate the theoretical energy $\mathcal{E}$ for the ground electric subband in a rectangular $\text{Ga}_{0.67}\text{Al}_{0.33}\text{As}/\text{GaAs}/\text{Ga}_{0.67}\text{Al}_{0.33}\text{As}$ QW as a function of the well width d. Next we define the value of k_{z0} by the equality: $\mathcal{E}(d)=\hbar^2 k_{z0}^2/2m_0^*$, where $m_0^*=0.0660\ m_0$. This value of $k_{z0}=(2m_0^*\mathcal{E}/\hbar^2)^{1/2}$ is introduced to the above relations for g^*. When describing the final results for the g^* value and the cyclotron mass in QW we will use the same range of well widths.

In Fig. 2 we plot the spin g^* value of the conduction electrons in bulk GaAs as a function of d (or k_{z0}). The solid line indicates the exact values of g^* within 3LM, as obtained from Eqs. (11) and (12) for $B=2$ T. The free-electron and distant band contributions are kept only for the conduction band. The dashed line indicates values obtained from Eq. (17), resulting from the expansion for weak nonparabolicity. As can be expected, for bigger widths d (or smaller values of k_{z0}) the approximated values approach the exact ones. Finally, the dashed line marked with IK indicates values obtained from Eq. (9) of Ref. 3 with the use of the same material parameters. It can be seen that Ref. 3 predicts a much stronger dependence of g^* on k_{z0} than both our curves and, in particular, our dashed curve which has been calculated in the same nonparabolic approximation as that used in Ref. 3. The reason of this discrepancy is that the formulas given in Ref. 3 correspond to our Eq. (17), with our $2m_0/m_0^*$ replaced by $-2E_P(1/G_0+2/E_0)/3$ and our g_0^* replaced by $-2E_P(1/G_0-1/E_0)/3$. In case of the mass the approximation used in Ref. 3 is not too bad since it misses only the term of
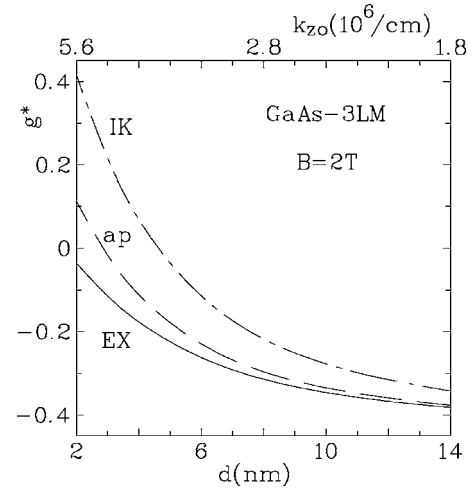

FIG. 2. Theoretical spin g^* factor of conduction electrons in bulk GaAs versus the wave vector k_{z0} parallel to the magnetic field **B**, or the corresponding well width d (see text). The solid line (EX) shows exact results from the three-level model, the dashed line (ap) represents the first nonparabolic approximation to 3LM, and the dashed-dotted line (IK) illustrates the results of Ref. 3 also based on 3LM (see text).

$1+C$ [cf. our Eq. (18)]. In case of the g^* value, however, it is seriously inadequate since it misses the additive term of $+2+2C'$, which is essential for the band-edge value of g_0^* in GaAs, see Eq. (19). As a result, the second term in the square bracket of Eq. (17) appears not with the coefficient $g_0^*=-0.44$, as it should, but with the coefficient of about -2.24. This gives a much too strong dependence of g^* on k_{z0}^2, as illustrated in Fig. 2.

The dependence of g^* on d (or k_{z0}), as given by the exact solution of 3LM (curve EX in Fig. 2), does not describe experimental data in $\text{GaAs}/\text{Ga}_{0.67}\text{Al}_{0.33}\text{As}$ quantum wells. In particular, it does not exhibit the change of sign to positive g^* factors for small values of d. On the other hand, we know that the inclusion of higher conduction Γ_7^v, Γ_8^v bands in the **P·p** description (see Fig. 1) results in stronger conduction band's nonparabolicity and, in particular, it gives the electron g^* values that change sign to positive at higher electron energies.[1] Thus it is necessary to include the Γ_7^c, Γ_8^c levels in the refined description of g^* in GaAs. This is equivalent to using the full matrix (8) for the determination of electron energies. In view of the applications to quantum wells the k_z terms must be retained. We pursue this program below.

B. Five-level model

In this section we calculate the spin g^* value of conduction electrons using the five-level **P·p** model. This model is adequate for the GaAs-type materials. Once the two upper conduction levels are included, the matrix elements P_1, Q, and $\bar{\Delta}$ come into play, see Fig. 1. As a result, two qualitatively new features appear. First, the appearance of the matrix element Q makes the conduction band nonspherical. Second, the matrix element Q does not vanish if the crystal is characterized by the BIA. This results in the spin splitting of conduction energies for a given direction of the wave vector

k (the Dresselhaus mechanism[5]). We develop a workable approach to the calculation of g^* factor in quantum wells based of 5LM using an iterative expansion in powers of the interband matrix elements P_0, P_1, and Q. Clearly, it is necessary to check whether such an expansion is adequate. In other words, we should make sure that the expansion procedure gives the g^* values comparable with those obtained from the complete matrix(8). To this end we first solve the eigenenergy problem given by the **P·p** Hamiltonian (8) by an alternative method, first used by Evtuhov for the nonspherical valence bands of Ge.[14] As already mentioned, for spherical energy bands the solutions of the eigenenergy problem in the presence of a magnetic field are given in terms of simple harmonic oscillator functions. For not too strong deviations from band's sphericity we look for the envelope functions in the form of sums of harmonic oscillator functions with unknown coefficients

$$f_l(\mathbf{r}) = \exp(ik_z z) \sum_{m=0} c_m^l |m>. \tag{20}$$

Since our Hamiltonian (8) contains raising and lowering operators for the harmonic oscillators, it is possible to perform the prescribed operations. Then we multiply the obtained eigenenergy equations on the left by consecutive harmonic oscillator functions and integrate the scalar products using the orthonormality relations. This results in equations for the coefficients and the condition for nontrivial solutions gives the eigenenergies. In other words, the Evtuhov method is a standard way of transforming a differential eigenvalue problem into an algebraic problem by taking for the complete set of functions the harmonic oscillator functions.

Not going into details of the procedure we will give a general scheme for the resulting eigenenergy matrix. The elementary irreducible block is a 7×7 matrix, one containing the spin-up state and another the spin-down state. If Q and k_z terms are neglected, the big matrix factorizes into the 7×7 matrices for the spin-up and spin-down energies for consecutive Landau levels. The nondiagonal Q and k_z terms couple the elementary 7×7 matrices. We find that in order to obtain precise energies for the lowest Landau levels we need to go to 70×70 matrices. The schematic form of such a matrix is given in Eq. (21).

$$
\begin{bmatrix}
N-1,- & Q\sqrt{B} & 0 & Qk_z & 0 & 0 & 0 & Pk_z & 0 & 0 \\
 & N,+ & Q\sqrt{B} & Pk_z & Qk_z & 0 & 0 & Qk_z & 0 & 0 \\
 & & N+3,- & Qk_z & Pk_z & Qk_z & Q\sqrt{B} & 0 & 0 & 0 \\
 & & & N+1,- & Q\sqrt{B} & 0 & 0 & Q\sqrt{B} & 0 & 0 \\
 & & & & N+2,+ & Q\sqrt{B} & Qk_z & 0 & 0 & 0 \\
 & & & & & N+5,- & Pk_z & 0 & Qk_z & Q\sqrt{B} \\
 & & & & & & N+4,+ & 0 & Q\sqrt{B} & Qkz \\
 & & & & & & & N-2,+ & 0 & \\
 & & & & & & & & N+7,- & Pk_z \\
 & & & & & & & & & N+6,+
\end{bmatrix}. \tag{21}
$$

We use a symbolic notation, for example, $N,+$ stands for the elementary 7×7 matrix containing the conduction Landau level n with spin up. The symbols Pk_z and Qk_z stand for 7×7 matrices containing $P_0 k_z$, $P_1 k_z$, and Qk_z terms, respectively, while $Q\sqrt{B}$ stands for 7×7 matrices containing $Q\sqrt{B}$ terms.

To calculate the g^* value we will be interested in the lowest conduction levels $0^\pm$. For $N=0$, matrix (21) gives the energy of the conduction level 0^+ (second row and column) perturbed by interactions with other levels. For $N=1$ we obtain the energy of the 0^- level (first row and column). Fixing the values of B and k_z we obtain from matrix (21) the energies which we consider to be "exact," so we use them as standards in the estimation of following expansions.

Next we turn back to the set of 14 equations for the envelope functions f_l, as given by the initial differential matrix (8). We find the envelope functions by substitution using an iteration procedure. In the first step we put $Q=0$ and express 12 envelope functions by f_4 and f_{11}, corresponding to the spin-up and spin-down Γ_6^c conduction states. Next the Q terms are restored and the zero-order functions are put back to the complete equations. The 12 first-order f_l functions are expressed by f_4 and f_{11}. In this approximation, linear in Q terms, the BIA (Dresselhaus) spin splitting is included. Finally, we return again to the initial set and determine the 12 functions f_l by f_4 and f_{11} including the Q^2 terms. The resulting equations for f_4 and f_{11} represent the effective Hamiltonian. It is obtained in the form of a 2×2 differential matrix since the bulk inversion asymmetry mixes the two spin states.

We are now in a position to calculate electron energies and the resulting conduction g^* factor for given values of B and k_z (still for the bulk). In the obtained formulas for energies there appear k_z, k_z^2, and k_z^4 terms. We checked that the k_z
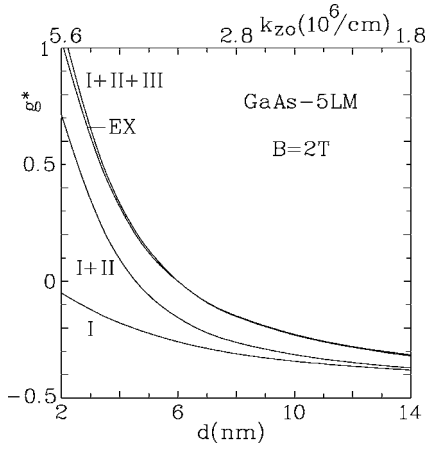
FIG. 3. Theoretical spin g^* factor of conducting electrons in bulk GaAs versus the wave vector k_{z0}, or the corresponding well width d (see text), as calculated from the five-level model. I, results for $Q=0$ (first iteration step); I+II, bulk inversion asymmetry included (linear Q terms, second iteration step); I+II+III, quadratic Q terms included (third iteration step). The line marked EX shows exact results calculated numerically for the bulk by the Evtuhov method.

and k_z^4 terms have negligible influence on the final energies.

In Fig. 3 we plot the calculated g^* values as functions of d (or k_{z0}) for the three consecutive approximations. To determine k_{z0} for a given width d we use the same procedure as described before (cf. Fig. 2). Our three approximations for the g^* value correspond to the three iteration steps. Curve I corresponds to $Q=0$, the corresponding formulas contain P_0^2 and P_1^2 type of terms. Curve I+II includes the previous approximation plus the terms $P_0 P_1 Q$, $\bar{\Delta} P_0^2 Q$, $\bar{\Delta} P_1^2 Q$, accounting for the spin splitting due to BIA. Curve I+II+III includes the two previous approximations plus the terms $P_0^2 Q^2$, $P_1^2 Q^2$, $\bar{\Delta} P_0 P_1 Q^2$ (the last terms are very small and may be neglected). In the same Fig. 3 we plot the g^* value obtained from the exact numerical procedure based on matrix (21).

A discussion of the results shown in Fig. 3 is in order. First, curve I gives the results very similar to those marked by EX in Fig. 2. Although the calculation I includes the higher conduction levels, as compared to 3LM used for EX, it turns out that the results of 3LM and 5LM with $Q=0$ are very similar if one adjusts C and C' constants to have the same band-edge values of m_0^* and g_0^*. Second, a sizable difference between the calculations I and I+II may appear unexpected. Compared to I, the calculation I+II includes the Dresselhaus spin splitting due to BIA, which is usually rather small. Indeed, for relatively large d (small k_{z0}) the corrections due to BIA are small. It is at small widths d (large k_{z0}) that they become appreciable. One should keep in mind that BIA works directly on the spin splitting, i.e., on the g^* value. More generally, the BIA spin splitting has somewhat particular properties since, while it is *affected* by a magnetic field, its primary origin is *not* a magnetic field. Finally, it follows from Fig. 3 that the curve I+II+III almost coincides with the exact result. This means that the third step in the iteration procedure gives enough precision in the calculation of the

electron g^* value. We use this information in the following treatment of the spin splitting in quantum wells.

III. g^* FACTOR AND CYCLOTRON MASS IN QUANTUM WELLS

We apply the above results to calculation of the spin g^* factor for conduction electrons in QWs grown along the **z** direction. We use 5LM and consider both the growth direction and a magnetic field parallel to the [001] crystal axis. Matrix (8) must now be completed by the potential $V(z)$ in all diagonal terms. The calculation is carried out by iterating solutions of Eq. (8), as described above for the bulk. The difference is that now we keep the operator $\hat{p}=(\hbar/i)\partial/\partial z$ in the differential form since the envelope functions in QWs are unknown and they must be determined by solving the eigenenergy problem. As a consequence, it is necessary in the iteration procedure to observe the order of z-dependent terms. In our treatment we keep the free-electron and far-band contributions only in the conduction band. While a more general treatment is possible, it makes the final formulas very lengthy while the precision is not markedly higher.

After a considerable manipulation the effective Hamiltonian for the spin-up and spin-down electron states in the conduction band is obtained in the form

$$\hat{H} = \begin{bmatrix} \hat{A}^+ & \hat{K} \\ \hat{K}^\dagger & \hat{A}^- \end{bmatrix}, \qquad (22)$$

where

$$\hat{A}^+ = V(z) - \frac{\hbar^2}{2}\frac{\partial}{\partial z}\frac{1}{m_I^*(\mathcal{E},z)}\frac{\partial}{\partial z} + \frac{P_x^2 + P_y^2}{2m_I^*(\mathcal{E},z)} + \frac{\mu_B B}{2}g_I^*(\mathcal{E},z)$$

$$+ \left(\frac{\hbar^2}{2m_0}\right)^2 \frac{E_Q}{3\hbar^2}\left\{\frac{\partial}{\partial z}[E_{P_0}(K_1 P_- P_+ + K_2 P_+ P_-)\right.$$

$$+ E_{P_1}(K_3 P_- P_+ + K_4 P_+ P_-)]\frac{\partial}{\partial z}$$

$$- \frac{2}{\hbar^2}[E_{P_0}(K_5 P_- P_+ P_- P_+ + K_6 P_+^2 P_-^2 + K_7 P_-^2 P_+^2)$$

$$\left.+ E_{P_1}(K_8 P_- P_+ P_- P_+ + K_9 P_+^2 P_-^2 + K_{10} P_-^2 P_+^2)]\right\}, \qquad (23)$$

$$\hat{A}^- = V(z) - \frac{\hbar^2}{2}\frac{\partial}{\partial z}\frac{1}{m_I^*(\mathcal{E},z)}\frac{\partial}{\partial z} + \frac{P_x^2 + P_y^2}{2m_I^*(\mathcal{E},z)} - \frac{\mu_B B}{2}g_I^*(\mathcal{E},z)$$

$$+ \left(\frac{\hbar^2}{2m_0}\right)^2 \frac{E_Q}{3\hbar^2}\left\{\frac{\partial}{\partial z}[E_{P_0}(K_1 P_+ P_- + K_2 P_- P_+)\right.$$

$$+ E_{P_1}(K_3 P_+ P_- + K_4 P_- P_+)]\frac{\partial}{\partial z}$$

$$- \frac{2}{\hbar^2}[E_{P_0}(K_5 P_+ P_- P_+ P_- + K_6 P_-^2 P_+^2 + K_7 P_+^2 P_-^2)$$

$$\left.+ E_{P_1}(K_8 P_+ P_- P_+ P_- + K_9 P_-^2 P_+^2 + K_{10} P_+^2 P_-^2)]\right\}. \qquad (24)$$

The effective mass is

$$\frac{m_0}{m_I^*(\mathcal{E},z)} = 1 + C - \frac{1}{3}\left[E_{P_0}\left(\frac{2}{\widetilde{E}_0} + \frac{1}{\widetilde{G}_0}\right) + E_{P_1}\left(\frac{2}{\widetilde{G}_1} + \frac{1}{\widetilde{E}_1}\right) \right.$$

$$\left. + \frac{4\bar{\Delta}\sqrt{E_{P_0}E_{P_1}}}{3}\left(\frac{1}{\widetilde{E}_1\widetilde{G}_0} - \frac{1}{\widetilde{E}_0\widetilde{G}_1}\right)\right], \qquad (25)$$

and the g^* factor is

$$g_I^*(\mathcal{E},z) = 2 + 2C' + \frac{2}{3}\left[E_{P_0}\left(\frac{1}{\widetilde{E}_0} - \frac{1}{\widetilde{G}_0}\right) + E_{P_1}\left(\frac{1}{\widetilde{G}_1} - \frac{1}{\widetilde{E}_1}\right) \right.$$

$$\left. - \frac{2\bar{\Delta}\sqrt{E_{P_0}E_{P_1}}}{3}\left(\frac{2}{\widetilde{E}_1\widetilde{G}_0} + \frac{1}{\widetilde{E}_0\widetilde{G}_1}\right)\right], \qquad (26)$$

where

$$\widetilde{E}_i = E_i - \mathcal{E} + V(z), \qquad (27)$$

$$\widetilde{G}_i = G_i - \mathcal{E} + V(z). \qquad (28)$$

We use the notation $E_{P_0}=2\hbar^2 P_0^2/m_0$, $E_{P_1}=2\hbar^2 P_1^2/m_0$, and $E_Q=2\hbar^2 Q^2/m_0$. Further

$$K_1 = \frac{1}{3\widetilde{G}_1}\left(\frac{26}{\widetilde{G}_0\widetilde{E}_0} + \frac{5}{\widetilde{G}_0^2} + \frac{5}{\widetilde{E}_0^2}\right),$$

$$K_2 = \frac{1}{\widetilde{E}_0^2}\left(\frac{8}{\widetilde{E}_1} + \frac{1}{\widetilde{G}_1}\right) + \frac{1}{\widetilde{G}_1\widetilde{G}_0}\left(\frac{2}{\widetilde{E}_0} + \frac{1}{\widetilde{G}_0}\right),$$

$$K_3 = \frac{1}{3\widetilde{E}_0}\left(\frac{26}{\widetilde{G}_1\widetilde{E}_1} + \frac{5}{\widetilde{G}_1^2} + \frac{5}{\widetilde{E}_1^2}\right),$$

$$K_4 = \frac{1}{\widetilde{G}_1^2}\left(\frac{8}{\widetilde{G}_0} + \frac{1}{\widetilde{E}_0}\right) + \frac{1}{\widetilde{E}_1\widetilde{E}_0}\left(\frac{2}{\widetilde{G}_1} + \frac{1}{\widetilde{E}_1}\right),$$

$$K_5 = \frac{1}{3\widetilde{G}_1}\left(\frac{1}{\widetilde{E}_0} - \frac{1}{\widetilde{G}_0}\right)^2,$$

$$K_6 = \frac{1}{2\widetilde{E}_0^2}\left(\frac{1}{\widetilde{E}_1} + \frac{2}{\widetilde{G}_1}\right),$$

$$K_7 = \frac{1}{2}\left(\frac{2}{\widetilde{G}_1\widetilde{G}_0^2} + \frac{1}{\widetilde{E}_1\widetilde{E}_0^2}\right),$$

$$K_8 = \frac{1}{3\widetilde{E}_0}\left(\frac{1}{\widetilde{E}_1} - \frac{1}{\widetilde{G}_1}\right)^2,$$

$$K_9 = \frac{1}{2\widetilde{G}_1^2}\left(\frac{1}{\widetilde{G}_0} + \frac{2}{\widetilde{E}_0}\right),$$

$$K_{10} = \frac{1}{2}\left(\frac{2}{\widetilde{E}_0\widetilde{E}_1^2} + \frac{1}{\widetilde{G}_0\widetilde{G}_1^2}\right). \qquad (29)$$

We emphasize that the mass m_I^* and the g value g_I^* defined in Eqs. (25) and (26) do not represent the final cyclotron mass and g value in a quantum well but only the first iterative approximations to these quantities, as obtained from matrix (8) by setting $Q=0$.

The nondiagonal component in Eq. (22), related to the bulk inversion asymmetry, is

$$\hat{K} = \hat{B}_1 + \hat{B}_2, \qquad (30)$$

where

$$\hat{B}_1 = \frac{-\sqrt{2}}{\hbar}\gamma(\mathcal{E},z)\left[P_+\frac{\partial^2}{\partial z^2} + \frac{1}{4\hbar^2}(P_-P_+^2 + P_+^2 P_-)\right], \quad (31)$$

$$\hat{B}_2 = \frac{1}{\sqrt{2}\hbar^3}\gamma(\mathcal{E},z)P_-^3, \qquad (32)$$

in which

$$\gamma(\mathcal{E},z) = \frac{4Q}{3}\left\{ P_0 P_1\left(\frac{1}{\widetilde{G}_0\widetilde{G}_1} - \frac{1}{\widetilde{E}_0\widetilde{E}_1}\right) \right.$$

$$\left. - \frac{\bar{\Delta}}{3}\left[\frac{P_0^2}{\widetilde{E}_0\widetilde{G}_0}\left(\frac{2}{\widetilde{E}_1} + \frac{1}{\widetilde{G}_1}\right) - \frac{P_1^2}{\widetilde{E}_1\widetilde{G}_1}\left(\frac{2}{\widetilde{G}_0} + \frac{1}{\widetilde{E}_0}\right)\right]\right\}. \qquad (33)$$

The diagonal components in the Hamiltonian (22) are composed of the terms proportional to P_0^2 and P_1^2, resulting from the first iteration step (marked I in the previous sections). They contain also the terms proportional to $P_0^2 Q^2$ and $P_1^2 Q^2$, resulting from the third iteration step (marked III). The diagonal terms neither raise nor lower the harmonic oscillator functions. The nondiagonal terms $\hat{B}_1$ and $\hat{B}_2$ are proportional to Q and they come from the second iteration step (marked II). They result from the bulk inversion asymmetry of the crystal. The operator $\hat{B}_1$ raises the harmonic oscillator function $|n>$ to $|n+1>$, whereas $\hat{B}_2$ lowers it from $|n>$ to $|n-3>$. In consequence, solving the eigenenergy problem imposed by Eq. (22) requires again the Evtuhov procedure. However, now we have to look for solutions in the form

$$F_l = \sum_{m=0}^{\infty} c_m^l |m> \chi_m(z), \qquad (34)$$

where $l=1,2$, the functions $|m> = A_m \exp(ik_x x)\Phi_m(y)$ are the same as for the bulk, but $\chi_m(z)$ are as yet unknown envelope functions describing the motion along the growth direction z. When applying the functions (34) we will limit them to the minimal coupling scheme. It can be seen from Eq. (22) that the spin-up state $|n,+>$ described by $\hat{A}^+$ interacts via the offdiagonal elements $\hat{B}_1$ and $\hat{B}_2$ with the spin-down states. In view of the above considerations it is clear that $|n,+>$ interacts via $\hat{B}_2$ with $|n+3,->$ and via $\hat{B}_1$ with $|n-1,->$. After performing the operations on the harmonic oscillator functions we obtain the following eigenenergy problem in the minimal coupling scheme:

$$\begin{pmatrix} \hat{A}_n^+ - \mathcal{E} & \hat{B}_{2,n} & \hat{B}_{1,n} \\ \hat{B}_{2,n}^\dagger & \hat{A}_{n+3}^- - \mathcal{E} & 0 \\ \hat{B}_{1,n}^\dagger & 0 & \hat{A}_{n-1}^- - \mathcal{E} \end{pmatrix} \begin{pmatrix} \chi_n(z) \\ \chi_{n+3}(z) \\ \chi_{n-1}(z) \end{pmatrix} = 0. \quad (35)$$

This set of coupled differential equations gives three energies, of which we are interested in $\mathcal{E}(n,+)$. A similar reasoning leads to the following set of differential equations containing the $|n,->$ state:

$$\begin{pmatrix} \hat{A}_{n-3}^+ - \mathcal{E} & 0 & \hat{B}_{2,n} \\ 0 & \hat{A}_{n+1}^+ - \mathcal{E} & \hat{B}_{1,n} \\ \hat{B}_{2,n}^\dagger & \hat{B}_{1,n}^\dagger & \hat{A}_n^- - \mathcal{E} \end{pmatrix} \begin{pmatrix} \chi_{n-3}(z) \\ \chi_{n+1}(z) \\ \chi_n(z) \end{pmatrix} = 0, \quad (36)$$

Here we are interested in $\mathcal{E}(n,-)$.

In the above matrices we use the following notation:

$$\hat{A}_n^+ = V(z) - \frac{\hbar^2}{2} \frac{\partial}{\partial z} \frac{1}{m_I^*(\mathcal{E},z)} \frac{\partial}{\partial z} + \frac{\hbar eB}{m_I^*(\mathcal{E},z)} (n + 1/2) + \frac{\mu_B B}{2} g_I^*(\mathcal{E},z)$$
$$+ E_Q \frac{\hbar \omega_c^0}{6} \left\{ \frac{\hbar^2}{2m_0} \frac{\partial}{\partial z} \left[E_{P_0} ((n+1)K_1 + nK_2) + E_{P_1} ((n+1)K_3 + nK_4) \right] \frac{\partial}{\partial z} \right.$$
$$\left. - \hbar \omega_c^0 \{ E_{P_0} [(n+1)^2 K_5 + n(n-1)K_6 + (n+1)(n+2)K_7] + E_{P_1} [(n+1)^2 K_8 + n(n-1)K_9 + (n+1)(n+2)K_{10}] \} \right\}, \quad (37)$$

$$\hat{A}_n^- = V(z) - \frac{\hbar^2}{2} \frac{\partial}{\partial z} \frac{1}{m_I^*(\mathcal{E},z)} \frac{\partial}{\partial z} + \frac{\hbar eB}{m_I^*(\mathcal{E},z)} (n + 1/2) - \frac{\mu_B B}{2} g_I^*(\mathcal{E},z)$$
$$+ E_Q \frac{\hbar \omega_c^0}{6} \left\{ \frac{\hbar^2}{2m_0} \frac{\partial}{\partial z} \left[E_{P_0} (nK_1 + (n+1)K_2) + E_{P_1} (nK_3 + (n+1)K_4) \right] \frac{\partial}{\partial z} \right.$$
$$\left. - \hbar \omega_c^0 \{ E_{P_0} [n^2 K_5 + (n+1)(n+2)K_6 + n(n-1)K_7] + E_{P_1} [n^2 K_8 + (n+1)(n+2)K_9 + n(n-1)K_{10}] \} \right\}, \quad (38)$$

$$\hat{B}_{1,n} = \gamma(\mathcal{E},z) \frac{\sqrt{2}}{L} \left(\sqrt{n+1} \frac{\partial^2}{\partial z^2} + \frac{(n+1)\sqrt{n+1}}{2L^2} \right), \quad (39)$$

$$\hat{B}_{2,n} = -\frac{\gamma(\mathcal{E},z)}{\sqrt{2}L^3} \sqrt{(n+3)(n+2)(n+1)} \quad (40)$$

in which $K_1, \ldots, K_{10}$ are again given by Eq. (29).

If one is interested in the lowest spin states $|0,\pm>$, sets (35) and (36) do not contain the $n-1$ and $n-3$ components and the eigenenergy problems reduce to the following two sets of coupled differential equations. For the $|0,+>$ state

$$\begin{pmatrix} \hat{A}_0^+ - \mathcal{E} & \hat{B}_{2,n} \\ \hat{B}_{2,n}^\dagger & \hat{A}_3^- - \mathcal{E} \end{pmatrix} \begin{pmatrix} \chi_0(z) \\ \chi_3(z) \end{pmatrix} = 0, \quad (41)$$

while for the $|0,->$ state

$$\begin{pmatrix} \hat{A}_1^+ - \mathcal{E} & \hat{B}_{1,n} \\ \hat{B}_{1,n}^\dagger & \hat{A}_0^- - \mathcal{E} \end{pmatrix} \begin{pmatrix} \chi_1(z) \\ \chi_0(z) \end{pmatrix} = 0. \quad (42)$$

In order to determine the cyclotron mass for the lowest levels we need to know in addition the energies of $|1,+>$ and $|1,->$ states. As follows from Eq. (36), for the $|1,->$ state the corresponding differential set still contains two equa-

tions, while for the $|1,+>$ state we have, in principle, three coupled equations, see Eq. (35). However, we found that the addition of the third state $|4,->$ [see Eq. (35)] does not really change the energy of the $|1,+>$ state, so that two equations suffice to determine its energy.

Once the electron is in a QW of a finite height, its total g^* factor is given not only by its properties in the well but also by those in the barriers. The situation for a rectangular GaAs/Ga$_{0.67}$Al$_{0.33}$As QW is shown in Fig. 4. Since the electron wave function penetrates into the barriers in which g^* is different from those in the well, we should average over the two regions. Seemingly, one should simply use the band-edge values of g^* in GaAs and Ga$_{0.67}$Al$_{0.33}$As and take an appropriate average. In fact, this was done in Ref. 3. We argue, however, that this is incorrect. The reason is that, as follows from Fig. 4, the electron energy is much lower than the barrier's band edge V_B. This effect is automatically included in our formalism if we use for both the well and the barriers the appropriate functions $\widetilde{E}_i$ and $\widetilde{G}_i$, as given by Eqs. (27) and (28), respectively. When considering the two regions we have to change not only the appropriate values of energy gaps and spin-orbit energies but also the potential $V(z)$. At the flat bottom of the well shown in Fig. 4, there is $V(z) = 0$. On the other hand, in the barrier region there is $V(z) = V_B$, where V_B is the offset value for the conduction
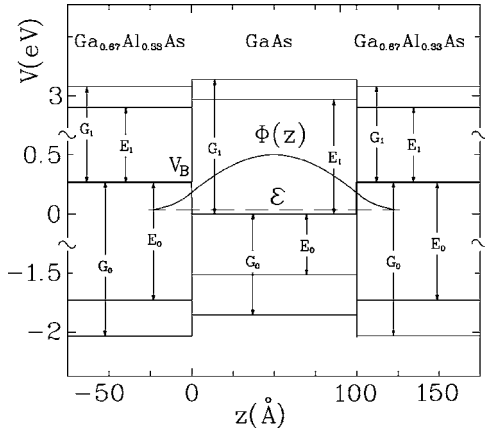
FIG. 4. Band structure of a rectangular GaAs/Ga$_{0.67}$Al$_{0.33}$As quantum well within 5LM along the growth direction z. The calculated energy and wave function of the ground subband is indicated.

band between the two materials. Clearly, the energy $\mathcal{E}$ is the same in the two regions. Only if V_B were zero would we deal with "straight" values of g^* in both materials.

It is instructive to consider a numerical example. Taking for Ga$_{0.67}$Al$_{0.33}$As the parameters given in Table I we obtain the band-edge value of $g_0^*=0.5378$, in agreement with the experimental findings.[13] On the other hand, when we compute the value of g^* in the barrier using the same parameters but accounting for $V_B=0.264$ meV and taking to a good approximation $\mathcal{E}\approx0$, we obtain $g^*=0.1638$, which is a considerably lower value.

In fact, in our formalism we do not employ the averaging procedure. When calculating the total electron g^* value we use in the expressions for $g_I^*(\mathcal{E},z)$, $m_I^*(\mathcal{E},z)$, and K_i, as given by Eqs (37), (38), and (29), the actual functions $\tilde{E}_i$ and $\tilde{G}_i$ for a given region. This includes $V(z)$ and the local values of band parameters. Thus the actual values of g_I^*, m_I^*, and K_i enter both the differential equations defined by Eq. (22), as

TABLE I. Band parameters of Ga$_{1-x}$Al$_x$As alloys for different chemical compositions x, as used in the calculations, see Refs. 13 and 15–18. Energies E_0, G_0, E_1, and G_1 are defined in Fig. 1, C and C' are far-band contributions to the band-edge values of m_0/m_0^* and g_0^*, respectively, see Eqs. (18) and (19). The interband matrix elements of momentum and of the spin-orbit interaction are taken to be independent of x: $E_{P_0}=27.865$ eV, $E_{P_1}=2.361$ eV, $E_Q=15.563$ eV, and $\bar{\Delta}=-0.061$ eV.

	GaAs	Ga$_{0.74}$Al$_{0.26}$As	Ga$_{0.67}$Al$_{0.33}$As
G_1(eV)	3.140	3.395	3.463
E_1(eV)	2.969	3.221	3.289
E_0(eV)	−1.519	−1.888	−1.992
G_0(eV)	−1.860	−2.199	−2.297
C	−2.297	−1.904	−2.248
C'	−0.025	−0.043	−0.056
V_B(eV)		0.208	0.264
m_0^*/m_0	0.066	0.0803	0.0875
g_0^*	−0.44	+0.40	+0.54

well as the boundary conditions at the interfaces. The problem of the boundary conditions was intensely discussed in the early days of heterostructure investigations, see Ref. 4. It will suffice to say here that our Eqs. (37) and (38) are written in the hermitian form, so that the boundary conditions are obtained in the form of continuity of the wave function and of electric current across the interfaces. The eigenenergy calculation is done for each spin separately so that, as follows from Eq. (22), also the boundary conditions depend on the spin. Since the effective equations for the energies contain only p_z^2 terms, the boundary conditions are not more complicated than those for a z-dependent effective mass. Once $\mathcal{E}_0^+$ and $\mathcal{E}_0^-$ are computed, the g^* value is determined using the definition (15).

All the above remarks apply also to the computation of the cyclotron mass. The mass value in barriers also contains the offset V_B. In the above numerical example for Ga$_{0.67}$Al$_{0.33}$As, instead of the band-edge value m_0^* =0.0875m_0 we deal with the value $m^*=0.0748m_0$ in the barrier. We emphasize that this feature is of importance even in the simplest calculation of the energy and of the effective mass in a QW made of two materials. The above problem is recognized in the work of Bastard et al.[19,20] as well as in our earlier papers.[21,22]

IV. RESULTS AND DISCUSSION

Figure 5 shows our calculation of the electron spin g^* factor in GaAs/Ga$_{0.67}$Al$_{0.33}$As rectangular QWs together with available experimental data. This is the main result of our work. It can be seen that the complete five-level **P·p** model gives an excellent description of the g^* value as a function of the well width between 3 and 21 nm. In particular, the theory reproduces the experimental value of g^*=0 for the well width of 6 nm, as observed by Le Jeune et al.[23] In the discrepancy of the experimental points around d ≈4.5 nm, priority should be given to Ref. 23 (the circle) since the Raman data of Ref. 24 (the triangle) do not determine the conduction g^* value directly. Our calculation is carried out for the growth direction **z**∥[001] with an external magnetic field parallel to this direction. In order to reach the good description of experiments we had to use the full five-level model of the band structure, as discussed above. The theory agrees perfectly well with the experimental g^* value even for $d\approx30$ Å. One could find it surprising that the **P·p** theory works so well on the scale of few interatomic distances in GaAs, but this result is in agreement with a more general experience that the **P·p** theory works better than it should. It can be seen that the total g^* value for narrow wells is smaller than the value for pure GaAs, as shown in Fig. 5. This is due to the above-mentioned effect of the offset V_B, which lowers the effective g^* in the barriers, as compared to the band-edge g^* value in Ga$_{0.67}$Al$_{0.33}$As.

The dashed line in Fig. 5 shows the calculation of the g^* factor, in which we used the three-level **P·p** model. This model does not involve the Q matrix element, so that it includes neither BIA splitting nor the Q^2 terms. It can be seen that 3LM does not properly describe the experimental data in GaAs/Ga$_{0.67}$Al$_{0.33}$As quantum wells. This result agrees with
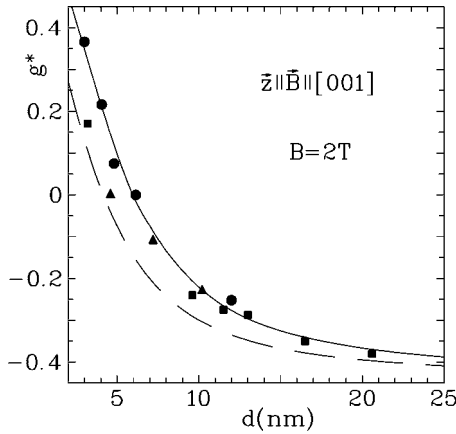
FIG. 5. Spin g^* factor of conduction electrons in rectangular GaAs/Ga$_{0.67}$Al$_{0.33}$As quantum wells versus well width d. The solid line, theory based on 5LM; the dashed line, theory based on 3LM; circles, data of Le Jeune et al. (Ref. [23]); triangles, data of Sapega et al. (Ref. [24]); squares, data of Malinowski et al. (Ref. [25]).

FIG. 6. Cyclotron mass of conduction electrons in rectangular GaAs/Ga$_{0.74}$Al$_{0.26}$As quantum wells versus well width d. The solid line, theory based on 5LM; the dashed line, theory based on 3LM; experimental data are after Huant et al. (Ref. [26]) for samples with slightly different chemical composition. Full circles $x=0.26$, full square $x=0.25$, full triangle $x=0.23$.

the general conclusion that the three-level model does not describe correctly the conduction band in GaAs-type materials, see Refs. [1] and [2]. The values of g^* shown in Fig. 5 were computed for the magnetic field intensity $B=2$ T. It is natural that in a theory for the nonparabolic energy band, when the energies are nonlinear functions of a magnetic field, the g^* value may depend somewhat on B. We checked this dependence and found that diminishing the field until $B \approx 0.25$ T the g^* value varies only weakly with B. However, as B tends to zero the g^* value ceases to be a useful quantity because of the spin splitting due to BIA. It is then more practical to use the energy splitting for the two spins.

As to the previous description of the g^* value in QW based on 3LM,[3] it is incorrect on two accounts. First, as already mentioned in the discussion of Fig. 2, it predicts a much too strong increase of g^* in GaAs with decreasing well width d. Second, when averaging the spin g^* factors in the GaAs well and Ga$_{0.67}$Al$_{0.33}$As barriers, it takes the band-edge values in both materials, neglecting the influence of the band offset on the g^* value in barriers. Both above shortcomings lead to an increase of the total g^*. We conclude that the agreement of the theory[3] with the experiment on GaAs/Ga$_{0.67}$Al$_{0.33}$As QW, as quoted by Le Jeune et al.,[23] is fortuitous.

In Fig. 6 we plot the cyclotron mass of electrons in GaAs/Ga$_{0.74}$Al$_{0.26}$As rectangular QWs as a function of the well width according to the three-level and five-level models. It can be seen that 3LM gives distinctly lower masses, although we adjust the far-band contribution C to get the same band-edge value of $m_0^*=0.0665m_0$. The five-level model gives slightly different masses for spin-up and spin-down cyclotron transitions.

Figure 6 shows the comparison of our theory with the cyclotron resonance data of Huant et al.[26] obtained on GaAs/Ga$_{1-x}$Al$_x$As QWs. For the GaAs/Ga$_{0.74}$Al$_{0.26}$As alloy we use the band parameters indicated in Table I. For the band edge in GaAs we take the perfectly acceptable value of $m_0^* =0.0665m_0$, accounting for the fact that the data of Ref. [26] were taken at the temperatures 20–30 K. Our theory de-
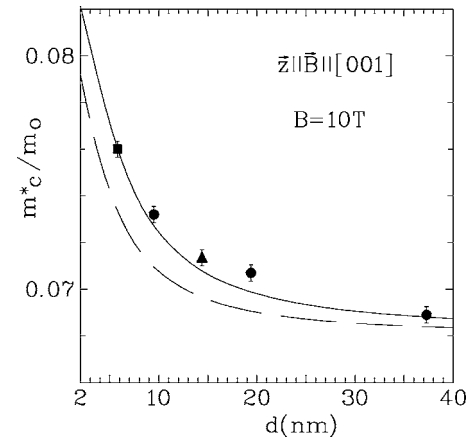
scribes the data very well with the exception of the point at $d \approx 20$ nm, but this point does not follow well the overall mass behavior. The calculation shown in Fig. 6 was performed for $B=10$ T, which corresponds to the experimental conditions of Ref. [26]. Comparing the data with the theory we conclude that the three-level model cannot correctly describe the experimental data.

The previous theoretical treatment of the effective masses in GaAs/Ga$_{1-x}$Al$_x$As QWs by Ekenberg,[4] which was carried out for $B=0$, makes a distinction between the masses parallel and perpendicular to the growth direction. We do not introduce the parallel mass since it does not seem to have a clear physical meaning. Also, in nonparabolic energy bands one cannot separate the electron motion in different directions since an increase of the mass due to motion in one direction will affect the motion in other directions. The theory of Ref. [4] is based on an expansion of the energy in powers of momentum.[27] The coefficients in such an expansion contain the band-edge energies in their denominators and the interband matrix elements of momentum in their numerators. In Ref. [4] the potential $V(z)$ of the well is added later, so that this procedure can be qualified as semiclassical. On the other hand, in our treatment we introduce the potential $V(z)$ and the energy $\mathcal{E}$ from the beginning and use the iteration procedure in solving the resulting 14 equations by substitution. This procedure is exact for the matrix element $Q=0$ and includes Q to second order. The resulting effective equations have the coefficients which not only contain the band-edge energies, but also involve in their denominators $V(z)$ and $\mathcal{E}$, cf. Eqs. (27)–(29). We showed above that these quantities are not negligible in GaAs-type materials and they would be even more important in narrow-gap materials. The work[4] does not include the bulk inversion asymmetry effects, which are not very important for the cyclotron mass but become important for the spin g^* value, see our Fig. 3. Our theoretical masses for GaAs/Ga$_{0.7}$Al$_{0.3}$As QW (not shown) are somewhat higher then those presented in Fig. 4 of Ref. [4]. It is not clear whether the differences result from the approxi-

mations made in Ref. 4 or from somewhat different band parameters used in the two calculations.

The approach presented above can be used equally well for quantum wells described by an arbitrary potential $V(z)$. This amounts to solving differential equations (22), (37), and (38), in which $V(z)$ explicitly appears. However, if a well (and a corresponding potential) does not possess the inversion symmetry, there appears a spin splitting due to the Bychkov-Rashba mechanism.[6] Technically, this appears as a result of noncommutativity of $\hat{p}_z$ with $V(z)$ when one solves the **P·p** equations by substitution. The Bychkov-Rashba splitting has been treated in many papers, see the review.[28]

The present work confirms our previous description of the spin g^* factor in parabolic GaAs/Ga$_{1-x}$Al$_x$As quantum wells.[29,30] We conclude that the five-level **P·p** model adequately describes this important system. The spin g^* factor in bulk GaAs was very recently described using the empirical tight binding approach.[31]

V. SUMMARY

We describe the spin and cyclotron energies of electrons in GaAs/Ga$_{1-x}$Al$_x$As quantum wells in the presence of an external magnetic field parallel to the growth direction [001]. Our approach is based on the five-level **P·p** model of a band structure for GaAs-type materials. Inadequacy of the previous theory used in the literature for the spin g^* factor in heterostructures is indicated. We solve 14 coupled differential equations resulting from the **P·p** formulation by three iteration steps. The sufficiency of this procedure is tested on bulk GaAs energies for different values of k_z^2 corresponding to real quantum wells. Influence of the bulk inversion asymmetry present in III-V compounds on the electron g^* value is emphasized. Our theory gives an excellent description of the existing experimental data on the spin g^* factor and the cyclotron mass of electrons in GaAs/Ga$_{1-x}$Al$_x$As rectangular quantum wells for different well widths.

*Corresponding author. Email address: pfeff@ifpan.edu.pl

[1] P. Pfeffer and W. Zawadzki, Phys. Rev. B **41**, 1561 (1990).

[2] P. Pfeffer and W. Zawadzki, Phys. Rev. B **53**, 12813 (1996).

[3] E. L. Ivchenko and A. A. Kiselev, Fiz. Tekh. Poluprovodn. (S.-Peterburg) **26**, 1471 (1992) [Sov. Phys. Semicond. **26**, 827 (1992)].

[4] U. Ekenberg, Phys. Rev. B **40**, 7714 (1989).

[5] G. Dresselhaus, Phys. Rev. **100**, 580 (1955).

[6] Y. A. Bychkov and E. I. Rashba, J. Phys. C **17**, 6039 (1984).

[7] R. Bowers and Y. Yafet, Phys. Rev. **115**, 1165 (1959).

[8] W. Zawadzki, in *Narrow Gap Semiconductors, Physics and Applications*, edited by W. Zawadzki (Springer, Berlin, 1980), p. 85.

[9] W. Zawadzki, in *Landau Level Spectroscopy*, edited by G. Landwehr and E. I. Rashba (North-Holland, Amsterdam, 1991), p. 483.

[10] M. Singh, P. R. Wallace, and S. Askenazy, J. Phys. C **15**, 6731 (1982).

[11] B. Lax, J. G. Mavroides, H. J. Zeiger, and R. J. Keyes, Phys. Rev. **122**, 31 (1961).

[12] W. Zawadzki, Phys. Lett. **4**, 190 (1963).

[13] C. Weisbuch and C. Hermann, Phys. Rev. B **15**, 816 (1977).

[14] V. Evtuhov, Phys. Rev. **125**, 1869 (1962).

[15] C. Bosio, J. L. Staehli, M. Guzzi, G. Burri, and R. A. Logan, Phys. Rev. B **38**, 3263 (1988).

[16] O. Berolo and J. C. Woolley, *Proceedings of the 11th International Conference of Physics on Semiconductors* (Polish Scientific Publishers, Warsaw, 1972), p. 1420.

[17] B. El Jani, P. Gibart, J. C. Portal, and R. L. Aulombard, J. Appl. Phys. **58**, 3481 (1985).

[18] M. Missous, in *Properties of Aluminium Gallium Arsenide*, edited by S. Adachi (Inspec, 1993), p. 75.

[19] G. Bastard, J. A. Brum, and R. Ferreira, in *Solid State Physics*, edited by H. Ehrenreich and D. Turnbull (Academic Press, New York, 1991), Vol. 44, p. 229.

[20] G. Bastard, *Wave Mechanics Applied to Semiconductor Heterostructures* (Les Editions de Physique, Les Ulis, 1988), p. 187.

[21] P. Pfeffer, Phys. Rev. B **55**, R7359 (1997).

[22] P. Pfeffer and W. Zawadzki, Phys. Rev. B **59**, R5312 (1999).

[23] P. Le Jeune, D. Robart, X. Marie, T. Amand, M. Brousseau, J. Barrau, V. Kalevich, and D. Rodichev, Semicond. Sci. Technol. **12**, 380 (1997).

[24] V. F. Sapega, T. Ruf, M. Cardona, K. Ploog, E. L. Ivchenko, and D. N. Mirlin, Phys. Rev. B **50**, 2510 (1994).

[25] A. Malinowski and R. T. Harley, Phys. Rev. B **62**, 2051 (2000).

[26] S. Huant, A. Mandray, and B. Etienne, Phys. Rev. B **46**, 2613 (1992).

[27] M. Braun and U. Roessler, J. Phys. C **18**, 3365 (1985).

[28] W. Zawadzki and P. Pfeffer, Semicond. Sci. Technol. **19**, R1 (2004).

[29] G. Salis, Y. Kato, K. Ensslin, D. C. Driscoll, A. C. Gossard, and D. D. Awschalom, Nature (London) **414**, 619 (2001).

[30] P. Pfeffer and W. Zawadzki, Phys. Rev. B **72**, 035325 (2005).

[31] Ch. Ammann, Ch. Strahberger, and P. Vogl, EPS21 Condensed Matter Division Conference, Dresden, 2006 (unpublished).